



The Fracture of Concrete due to Erosive Wear by High Velocity Water Flow[©]

A. W. MOMBER, R. KOVACEVIC and J. YE
University of Kentucky
Lexington, Kentucky 40506

Wear and erosion of concrete structures by high velocity water flow is a basic aspect of the durability of marine and water constructions. The mechanism of concrete failure in such constructions is not well understood. Using high velocity water jets for simulating the loading, the authors observed the general behavior of the material during failure and investigated the influence of water velocity and exposure time. The results show that the interface between hardened cement paste and aggregate grains plays the main role in the fracture process. The basic mechanism of material failure is the generation and propagation of cracks at this interface. It is found that a critical loading intensity, which is characterized by a threshold velocity and a threshold exposure time, must be achieved in order to induce the erosion process. Through mass removal measurements, a mathematical relation between both parameters and the erosion intensity is found. Using a computer program for simulating the hydrodynamics inside a crack, the water pressure and flow velocities in a model crack were calculated.

KEY WORDS

Concrete, Erosion, Fracture, Mechanics, Numerical Modeling, Water Flow

INTRODUCTION

The wear of concrete due to the attack of fast flowing water is a problem since this material is used for marine and hydraulic structures, pipe coating and channel walls (1). The first systematic investigations on the wear resistance of concrete in marine structures were carried out in the 1940s (2). The mechanisms which act in this case of loading can be subdivided into three events, i.e., direct action of the high velocity water flow, or erosion, which is the topic of the present paper; action of imploding gas bubbles in high velocity

flow, or cavitation; and action of suspended solid particles with high velocities, or abrasion.

The study of the literature related to these topics shows the following results on the behavior of concrete (2)-(8):

- The attack is a localized process
- the attack has a dynamic character
- the properties (hardness, weight) of the abrasive materials in the concrete are of importance
- the distribution of the aggregates in the concrete is of importance in the case of equal concrete strengths
- the concrete should contain a minimum of fine constituents for high resistance
- higher compressive strength often leads to higher resistance, but there is no general relation
- higher homogeneity of the mix leads to higher resistance
- high strength concrete and/or concrete strengthened with polymers has higher resistances
- there is a relation between compressive strength and other influencing parameters, such as curing
- higher water-cement ratio leads to reduced erosion resistance
- porosity and permeability of the concrete influence its resistance
- the fracture energy is in good relation with the resistance against abrasion
- no general theories exist to describe the behavior of concrete in the case of erosion, cavitation or abrasion
- the general destruction mode is not well understood
- the most important parameters to describe the regime of loading are water velocity and exposure time. No basic investigations have been carried out to investigate the influence of these parameters.

Concrete is an inhomogeneous material which consists of a matrix (hardened cement paste), inclusions (aggregate grains), and a system of pores (gel pores, capillary pores), cracks and interfaces, as illustrated in Fig. 1. The mechanical properties of these structural phases differ widely from each other. Reference (9) proposed a hierarchic system of three levels on which structural modeling of concrete can be ap-

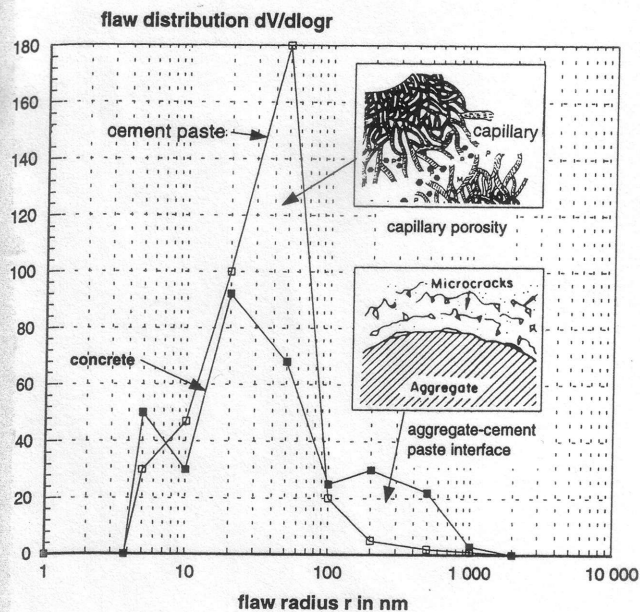


Fig. 1—Mercury intrusion porosimetry measurements on unloaded specimens of hardened cement paste and concrete.

plied, i.e., the micro-level, which is concerned with the structure of the hardened cement paste; the meso-level, which deals with pores, inclusions, cracks and interfaces; and the macro-level, which is related to the structural element (e.g. specimens). The basis of the present investigation is the assumption that the material characteristics of the meso-level, like pores, inclusions (aggregates), cracks and interfaces (between aggregates and cement matrix), are preferred objects for the penetration of fluids and strongly influence the behavior of concrete in the case of erosion by high velocity water flow.

MATERIALS AND EXPERIMENTAL METHODS

Materials

To investigate the influence of the aggregate particles, including their interfaces with the cement matrix, two different materials, a hardened cement paste and a concrete material, were designed and investigated. The cement paste is a hardened mixture of water (W) and a binding agent (B) in the ratio of $W/B = 0.55$. For the latter a PZ 35 F cement according to DIN 1164, was used. After mixing, this composition was cured and hardened for 28 days. The same procedure was followed for the concrete samples. In this case, the mixture consisted of water (W), binding agent (B) and limestone grains (G) as aggregates. The relation between water and binder was changed depending on the moisture absorbing capacity of the grain fractions to obtain comparable cement paste structures. The sample size was $150 \text{ mm} \times 150 \text{ mm} \times 150 \text{ mm}$.

Testing Equipment and Performance

The high speed water flow attack is simulated by a water jet impact with velocities up to 400 m/s. More details of jet generation, structure and action are found in Ref. (10). The high velocity water jet unit consists of a high pressure water pump (110 kW), hose system, nozzle holder, nozzle, and ro-

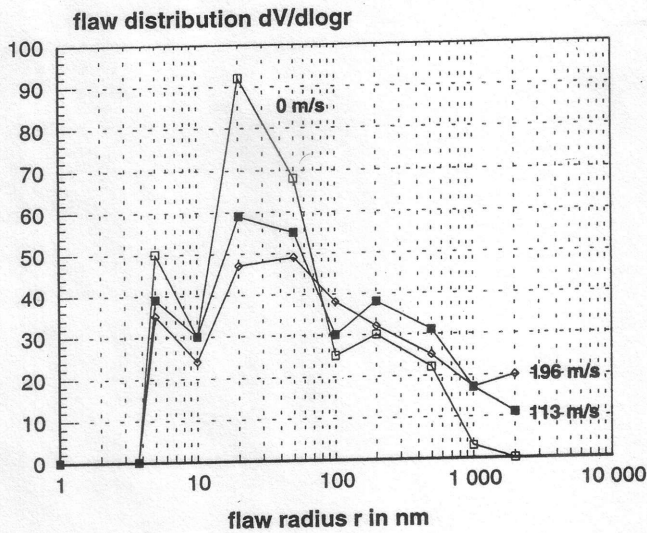
tating worktable. The nozzle holder and specimens are located inside a closed plexiglass cell, so that it is possible to collect the removed material and weigh it.

The pore and crack systems of the materials, including non-visible structural changes inside the specimens, are detected by a mercury penetration unit, shown in Fig. 1. Using the so called Washburn Equation, one can assume a relation between the pressure which is necessary to transport mercury into the structure and the size of the transport ways (pore-crack network). The sample size was $8 \text{ mm} \times 8 \text{ mm} \times 40 \text{ mm}$. The processes of preparation and handling are described in Refs. (11) and (12). Additionally, all samples and the removed materials were observed using optical and SEM microscopy.

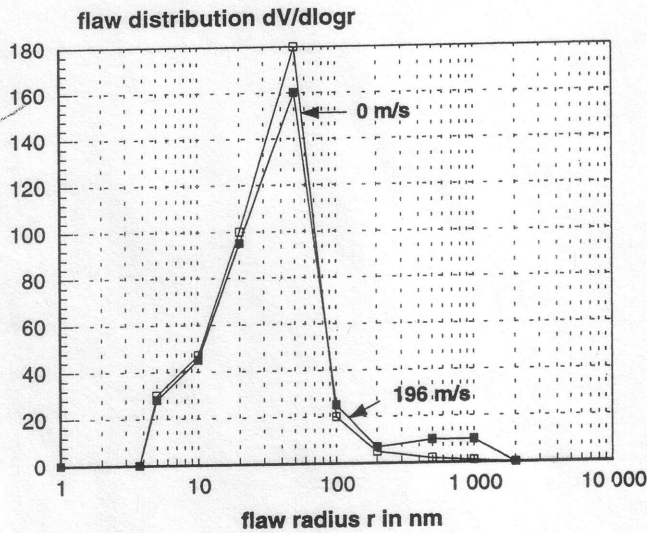
DESTRUCTION AND FAILURE PROCESS

Figures 1 and 2 show results of the mercury penetration measurements on plain and eroded samples. All measurements were carried out on undamaged areas of the specimens. In Fig. 1, one can find the differential flaw distributions of uneroded specimens. The flaw distribution curve for the plain cement matrix exhibits a maximum between 10 nm and 100 nm which is typical for this material and represents the capillary pore system. The addition of aggregates leads to a rising portion of larger flaws in the range between 100 nm and 1000 nm. This range is defined as a microcrack region (11) and describes the influence of the interfaces between cement paste and aggregate grains. In Refs. (13) and (14) it is shown that this interfacial zone is characterized by a high degree of microporosity, microcracking and reduced strength properties, and that it can be considered the weakest link in concrete with respect to strength. Here, the flaw radius r is identical to the crack width (11). Figure 2(a) shows the influence of the flow velocity on the differential flaw distributions of the eroded concretes. It can be noted that the amount of microcracks (widths between 100 nm and 1000 nm) but also of cracks with widths larger than 1000 nm rises significantly. One can therefore assume that a network of microcracks is formed before the visible macroscopic erosion process starts. These events can be described as an incubation period. Only the connection of these microcracks yields a measurable erosion and leads to the removal of single material grains.

The behavior of the plain cement paste, which is shown in Fig. 2(b), is somewhat different. The second maximum of the flaw distribution curve in the crack width range between 100 nm and 1000 nm is not very significant, therefore a network of microcracks is not expected. Figure 3, which shows a smooth macroscopic surface in the upper range of a failed cement paste sample, supports this conclusion. This material fails suddenly as a result of the presence of only a few large cracks. As shown in Ref. (15), a positive linear correlation exists between the critical effective crack length and the roughness of the fracture surface of cement paste and mortar, as shown in Fig. 4. Because the critical crack length is an indicator of the brittleness of quasibrittle materials, the roughness in the bottom region of the fracture surface of the cement paste specimen, shown on the left side of Fig. 3, de-



(a)



(b)

Fig. 2—Mercury intrusion porosity measurements on unloaded specimens (0 m/s) and specimens loaded by different flow velocities. (a) hardened concrete (b) hardened cement paste

scribes some late performances of energy absorption. The reason might be that nonhydrated cement clinkers are present to stop or branch the penetrating cracks. Also, the high roughness of the fracture surface of the concrete sample, shown on the right side of Fig. 4, indicates a high energy absorption during the material removal. These observations support the results and conclusions from the mercury intrusion porosimetry measurements.

INFLUENCE OF THE LOADING INTENSITY ON THE EROSIWE WEAR

Influence of the Water Flow Velocity

Using Bernoulli's law of pressure constancy:

$$g dh + \rho_f^{-1} dp + d(0.5 w^2) = \text{constant} \quad [1]$$

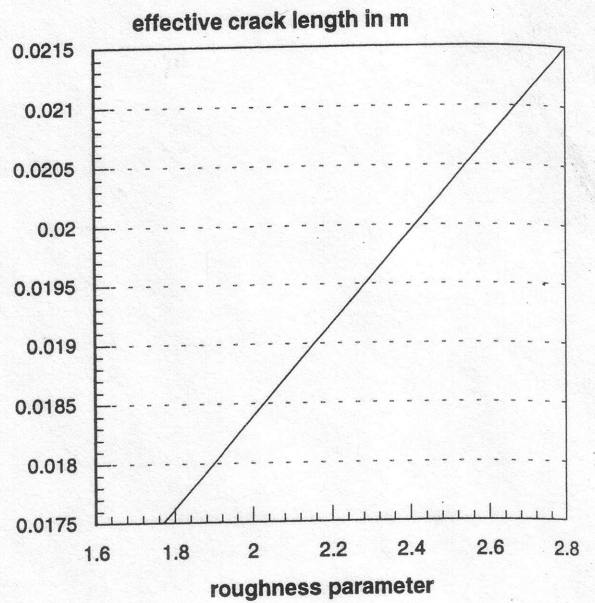
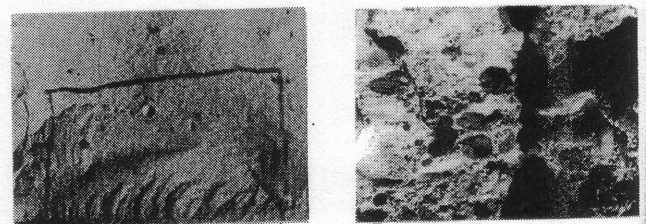


Fig. 3—Relation between fracture surface roughness parameter and effective crack length for hardened cement paste and mortar (15).



fracture surface of the hardened cement paste

fracture surface of a concrete sample

Fig. 4—Erosive fracture surface structures of specimens after water flow attack. left—hardened cement paste right—hardened concrete

the velocity of the water jet flow can be estimated by:

$$w_0 = \mu p_v \sqrt{2p_0/\rho_f} \quad [2]$$

Here, g is the gravity, h is the absolute height, ρ_f is the density of the fluid, p_0 is the static pressure and w_0 is the flow velocity. The parameters μ and p_v are reduction numbers and consider velocity losses due to friction on the nozzle walls and in the transport hoses, respectively. The factor μp_v was estimated to be 0.9. Figure 5 shows the relation between the fluid velocity w_0 and the mass loss due to erosion m . The function can be described by Eq. [3] as:

$$m = C_1 (w_0^2 - w_c^2) \quad [3]$$

The parameter w_c as the intersection between the abscissa and the function $m = f(w_0^2)$ can be taken as a critical threshold velocity which is needed to introduce the destruction of the material. As Fig. 5 shows, it depends on the type of material. It was found in water jet cutting investigations on rock (16) that this parameter was related to the stress intensity factor of the materials. The progress of the function,

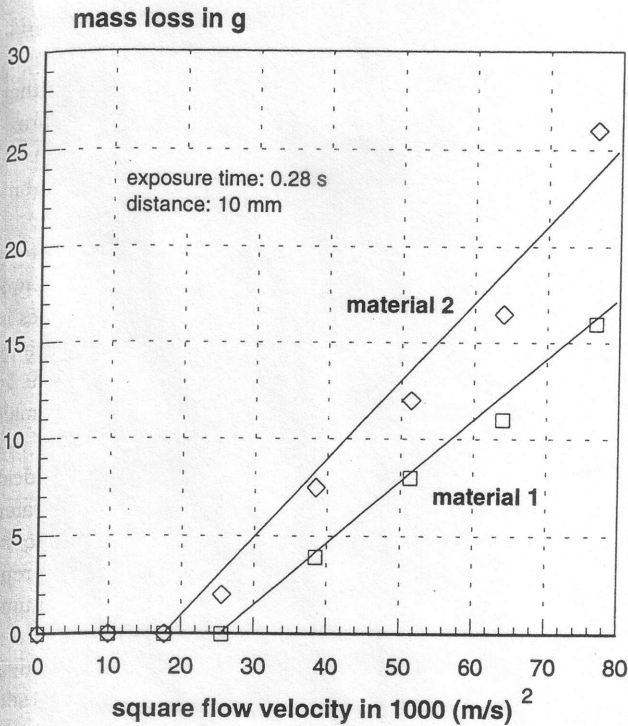


Fig. 5—Relation between water flow velocity and mass loss for two concrete mixtures.

$dm/d(w_0^2)$, also depends on the material, but it is constant over the whole velocity range for the given material. Contrary to the cement paste samples, the concrete specimens did not fail, but a continuous material removal was observed. This behavior illustrates again that unrestrained cracks could not be the source of the erosion. It could be assumed that the crack growth was interrupted due to events of energy dissipation and toughening mechanisms. Mechanisms related to the concrete can be crack shielding, crack deflection, crack arresting, crack bridging, and crack progress through aggregate grains (17). Several of these performances were observed during water jet cutting of concrete materials (18). Figure 6 shows details of the removal of single aggregate grains. The grain shown on the left side of Fig. 6 is completely intact so that it seems to be removed due to interfacial fracture which is connected with crack deflection and crack bridging. This assumption is supported by the SEM photograph of the concrete surface which shows the place where

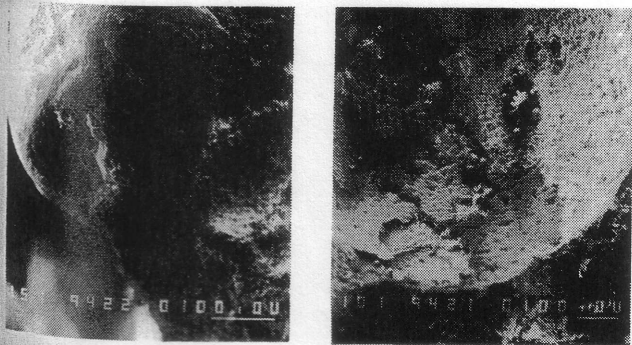


Fig. 6—SEM-photographs of a removed aggregate grain (left) and a selected concrete fracture surface area (right).

an aggregate grain was fixed prior to the material removal, shown on the right side of Fig. 6.

Influence of Exposure Time

The time of exposure, t , is simulated in this study by the traverse rate of the nozzle holder, v_T , and is calculated using Eq. [4]:

$$v_T = dx/dt ; \quad t = \int_0^{d_n} \frac{1}{v_T} dx \quad [4]$$

$$t = d_n/v_T \quad [5]$$

Here, d_n is the nozzle diameter and x is the traverse direction. In Fig. 7, the exposure time-mass loss relation is plotted based on Eq. [5]. It was found in this study, that the relation could be described by Eq. [6]:

$$m = m_0 \{1 - \exp[-(t + t_c)/t_1]\} \quad [6]$$

One can notice a threshold exposure time, t_c , on the intersection between the abscissa and the function $m = f(t)$. This minimum time is necessary to induce damage in the material. In Ref. (19), it is suggested that the critical threshold time can be related to the crack velocity of the material. Figure 7 also shows that the function asymptotically approaches a maximum value m_0 , which is identical to the mass loss in the case of stationary erosion ($t = \infty$). The role of the parameter t_1 is not yet clear. It seems that this parameter characterizes an exposure time related to the beginning of the decrease of the material removal progress.

Estimation of an Erosion Equation

As found in Ref. (19), a dependence between exposure time and jet velocity exists. From test results, the authors es-

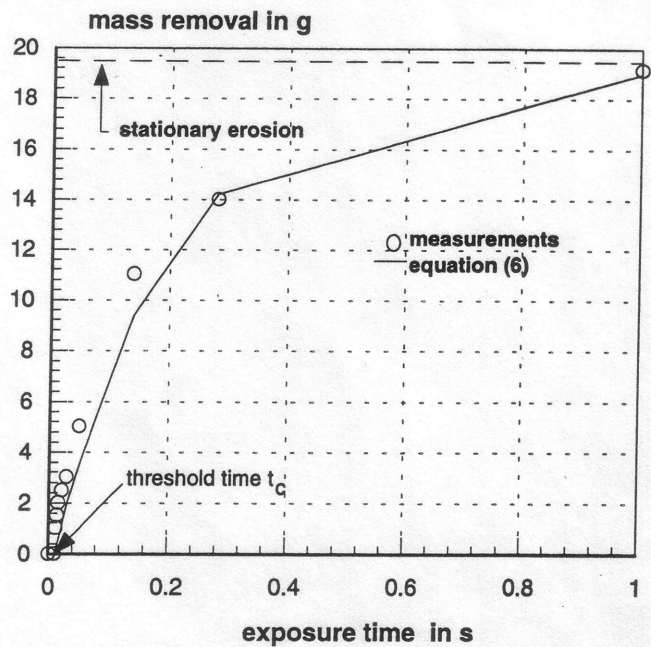


Fig. 7—Relation between exposure time and mass loss for a concrete mixture (water flow velocity: 235 m/s).

timated a relation according to Eq. [7] below:

$$w_c = at^{-b} \quad [7]$$

This relation is in good agreement with experimental data in Ref. (20). It was also found that the constant C_1 in Eq. [3] was independent of exposure time and traverse velocity, respectively, which corresponds with observations in high velocity abrasive wear investigations (21). Using Eqs. [3] and [7], the material mass loss due to high velocity water flow erosion can be calculated by Eq. [8] as:

$$m = C_1 [w_0^2 - (at^{-b})^2] \quad [8]$$

Figure 8, which is the graphical interpretation of this equation for selected mass loss values, shows that a minimum flow velocity is needed to start the erosion of the investigated concrete mixture ($m > 0$). The figure also illustrates the dominating influence of the flow velocity on the erosion performance.

NUMERICAL MODELING OF THE HYDRODYNAMICAL FRACTURE DURING EROSIVE WEAR

The experimental results show that the propagation of preexisting cracks is the main cause of erosive fracture of the material so that an analysis of the hydrodynamics inside a crack may lead to a better understanding of the erosion process.

The general situation in a separated crack and the fluid-dynamical basic equations for the modeling of the water flow

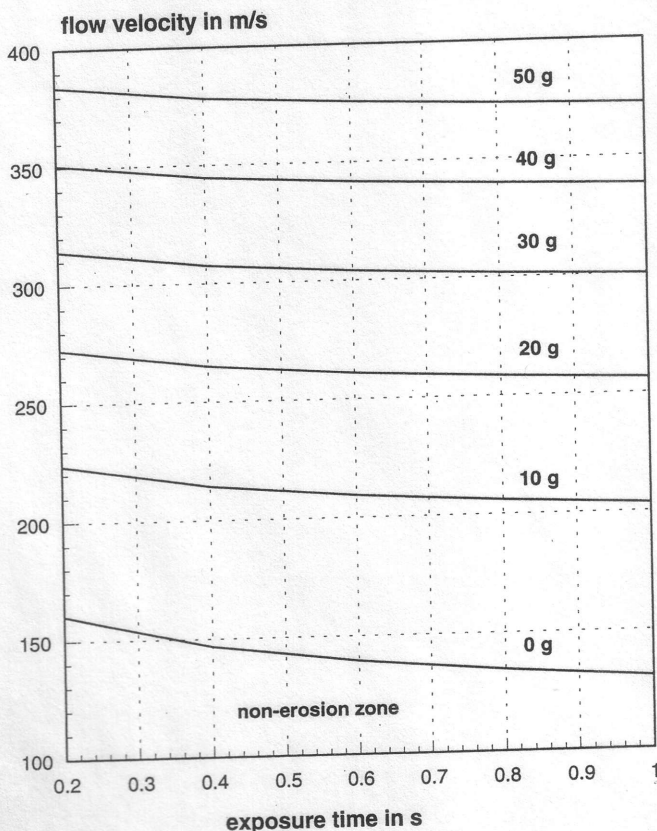
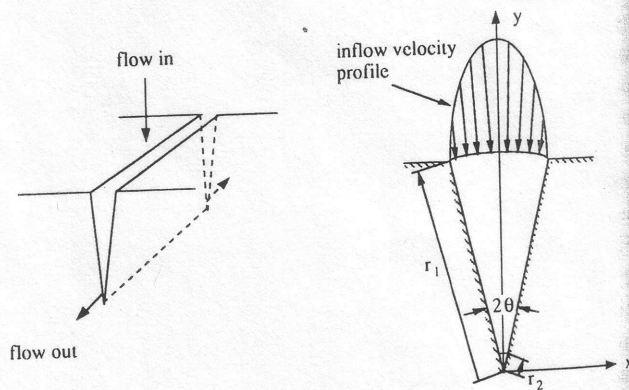


Fig. 8—Calculated mass loss values (m) for concrete using Eq. [8].

inside the crack are shown schematically in Fig. 9. In Ref. (22), an experiment is conducted to measure the main pressure produced by a water jet in a crack. The results show that the measured pressure at the bottom of the crack is approximately 23% of the jet pressure. In Ref. (23) a model is proposed for calculating the transient pressure in a crack, but the obtained results did not verify this method.

In the present work, it is assumed that the crack is a two-dimensional V-shaped region. The fluid flows between two intersecting stationary walls. The angle between the plates is 2θ . The inflow boundary is taken to be at the radius r_1 and the outflow boundary at the radius r_2 , as shown in Fig. 9. It is assumed a point sink which is approximated by a small channel near the point of intersection through which the fluid is discharged. This flow problem is similar to the ideal Hamel problem (24), but the inflow is caused by the water jet, and the plates are of finite length. The governing equations for the high speed water jet hitting a crack can be represented by the continuity equation and the momentum equation in the x and y directions, shown in Fig. 9, where u and v are the velocity components in the x and y directions, respectively, p is the pressure, ρ_f is the fluid density, and ν is the fluid kinetic viscosity. In the range of the material threshold velocity (< 140 m/s) the fluid is considered to be incompressible. For the numerical solution of the problem, a computer program based on the finite element method is used. As the calculations show, the flow velocity increases after the jet has entered the crack, as shown in Fig. 10. Further, the shape of the velocity profile changes with the crack length.



continuity equation

$$\frac{\partial \rho_f}{\partial t} + u \frac{\partial (\rho_f u)}{\partial x} + v \frac{\partial (\rho_f v)}{\partial y} = 0$$

momentum equations in x and y directions

$$\frac{\partial (\rho_f u)}{\partial t} + u \frac{\partial (\rho_f u)}{\partial x} + v \frac{\partial (\rho_f u)}{\partial y} = - \frac{\partial p}{\partial x} + \nu \left[\frac{\partial^2 (\rho_f u)}{\partial x^2} + \frac{\partial^2 (\rho_f u)}{\partial y^2} \right]$$

$$\frac{\partial (\rho_f v)}{\partial t} + u \frac{\partial (\rho_f v)}{\partial x} + v \frac{\partial (\rho_f v)}{\partial y} = - \frac{\partial p}{\partial y} + \nu \left[\frac{\partial^2 (\rho_f v)}{\partial x^2} + \frac{\partial^2 (\rho_f v)}{\partial y^2} \right]$$

Fig. 9—Model conditions and basic equations for the numerical simulation of the water flow in a model crack.

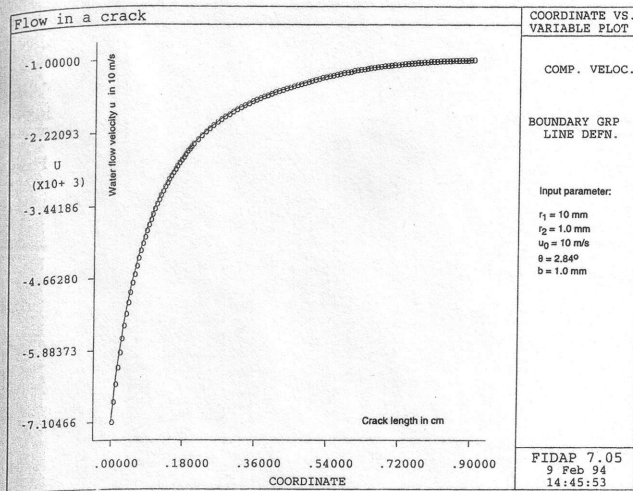


Fig. 10—Numerical solution of the water flow development inside a model crack.

Whereas the profile is comparable with a Gaussian curve at the entry zone of the crack, it becomes regular at the crack tip, as shown in Fig. 11. Near the bottom of the crack, the velocity reaches the maximum. During the sudden stoppage of the flow, forces will be generated due to momentum transfer. If these forces exceed critical values on the crack tip, the crack starts to grow.

CONCLUSIONS

The present investigation leads to the following conclusions:

1. A high speed water jet was used for the accelerated simulation of the concrete behavior in hydraulic structures.
2. The erosion of concrete by high velocity water flow is caused by the generation and widening of microcracks.
3. The erosion process starts in the interface between hardened cement paste and aggregate grains.
4. The erosion progress is controlled by toughening mechanisms, mainly caused by the aggregate-crack interaction.
5. A critical flow velocity w_c is needed to start the erosion process. This parameter is related to the fracture mechanical properties of the eroded material.
6. A critical exposure time t_c is also needed to start the erosion process. This parameter is related to the crack velocity in the eroded material.
7. The elementary process of the erosion is characterized by a water flow field in the attacked crack.
8. The process was investigated numerically using a hydro-mechanical model.

ACKNOWLEDGMENTS

The authors are thankful to the Alexander-von-Humboldt Foundation, Bonn, Germany, and to the Center for Robotics and Manufacturing Systems, University of Kentucky, Lexington, KY, for financial support. They also wish to thank the Institute of Material Sciences, University of Hannover, Germany, for supporting part of the experimental work.

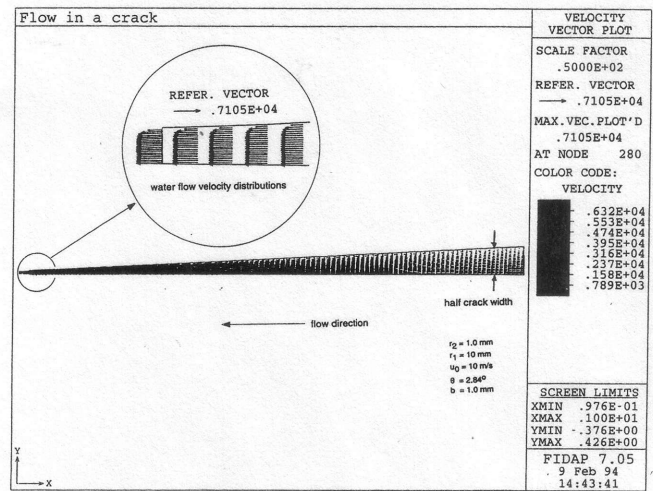


Fig. 11—Numerical solution for the water flow velocity distribution inside a model crack.

REFERENCES

- (1) Davis, A. P., "Save Velocities of Water in Concrete," *Eng. News*, pp 20-21, (1912).
- (2) Price, W. H., "Erosion of Concrete by Cavitation and Solids in Flowing Water," *Jour. of the ACI Proc.*, **43**, pp 1009-1023, (1947).
- (3) Walz, K. and Wischers, G., "On the Resistance of Concrete Against the Mechanical Action of High Speed Water," *Beton*, pp 403-405 and pp 457-460, (1969), (in German).
- (4) Pat, M. G. and Reinhardt, H. W., "Erosion of Concrete," *Heron*, **24**, pp 5-24, (1979).
- (5) Zhang, X. H. and Huang, Y., "Fundamental Study on the Abrasive Behavior of Concrete," in *Fracture Mechanics of Concrete*, Wittmann, F. H., ed., Elsevier, Amsterdam, (1983), pp 43-74.
- (6) Graham, J. R., "Erosion of Concrete in Hydraulic Structures," in *Manual of Concrete Practice*, Part 1, Amer. Concrete Inst., Detroit, (1988), pp R1-R22.
- (7) Mirza, J., Tureene, S. and Masounare, J., "Influence of Structural Parameters on the Abrasion-Erosion Resistance of Various Repairing Mortars," *Can. Jour. of Civil Eng.*, **17**, pp 12-17, (1990).
- (8) Dhir, R. K., Hewlett, P. C. and Chan, Y. N., "Near Surface Characteristics of Concrete: Abrasion Resistance," *Mat. and Struct.*, **24**, pp 122-128, (1991).
- (9) Wittmann, F. H., "Structure of Concrete With Respect to Crack Formation," in *Fracture Mech. of Concrete*, Wittmann, F. H., ed., Elsevier, Amsterdam, (1983), pp 43-74.
- (10) Momber, A., *Manual of Pressure Water Jets*, Beton-Verlag GmbH, Duesseldorf, (1993), pp 16-33, (in German).
- (11) Schneider, U. and Herbst, H. J., "Porosity Parameters of Concrete," *TIZ Int'l.*, **113**, pp 311-321, (1989), (in German).
- (12) Momber, A., "Mercury Intrusion Porosimetry Measurements on Concrete Samples Subjected by Pressure Water," *Materialwiss. und Werkstofftechnik*, **42**, pp 283-286, (1992), (in German).
- (13) Larbi, J. A., "Microstructure of the Interfacial Zone Around Aggregate Particle in Concrete," *Heron*, **38**, pp 3-69, (1993).
- (14) Alexander, M. G., "Two Experimental Techniques for Studying the Effects of the Interfacial Zone Between Cement Paste and Rock," *Cement and Concrete Res.*, **23**, pp 567-575, (1993).
- (15) Lange, D. A., Jennings, H. M. and Shah, S. P., "Relationship Between Surface Roughness and Fracture Behavior of Cement Paste and Mortar," *Jour. Amer. Ceram. Soc.*, **76**, 3, pp 589-597, (1993).
- (16) Wiedemeier, J., "High Speed Fluid Jets and the Fracture Mechanics of Brittle Materials," Ph.D. Dissertation, University of Hannover, Hannover, Germany, (1981), (in German).
- (17) Shah, S. P. and Ouyang, C., "Toughening Mechanisms in Quasi-Brittle Materials," *Jour. of Eng. Mat. and Tech.*, **115**, pp 300-307, (1993).
- (18) Momber, A. and Kovacevic, R., "On the Statistical Character of the Failure of Rocklike Materials Due to High Energy Water Jet," Ph.D. Dissertation, University of Hannover, Hannover, Germany, (1992).
- (19) Momber, A. and Kovacevic, R., "Fundamental Investigations on Concrete Wear by High Velocity Water Flow," Ph.D. Dissertation, University of Hannover, Hannover, Germany, (1993).

- (20) Erdmann-Jesnitzer, F., Louis, H. and Wiedemeier, J., "The Action of High Speed Water Jets on Materials—Measurement Methods and their Practical Application," in *Proc. 5th Int'l. Symp. Jet Cutting Tech.*, Stephens, H. S. and Jarvis, B., eds., (1980) pp 75–86.
- (21) Blickwedel, H., "Generation and Action of High Pressure Abrasive Jets," Ph.D. Dissertation, University of Hannover, Hannover, Germany, (1990), (in German).
- (22) Mazurkiewicz, M., Galecki, G. and White, J., "A Model Study of Water Pressure Distribution in a Crack When Impacted by a High-Pressure Water Jet," in *Proc. 8th Int'l. Symp. Jet Cutting Tech.*, Saunders, D., ed., (1986), pp 189–191.
- (23) Xu, J., "A New Model And Calculating Method of 'Water Wedge'," in *Proc. 9th Int'l. Symp. Jet Cutting Tech.*, Woods, P.A., ed., (1988), pp 659–666.
- (24) Batchelor, G. K., *An Introduction of Fluid Mechanics*, Cambridge Press, Cambridge, (1967).